Acta Cryst. (1998). B**54**, 485–493

Experimental Charge Density and Electrostatic Potential of Triglycine

Virginie Pichon-Pesme and Claude Lecomte*

LCM3B, Laboratoire de Cristallographie et Modélisation des Matériaux Minéraux et Biologiques, Université Henri Poincaré-Nancy 1, UPRESA CNRS 7036, Faculté de Sciences, BP 239, 54506 Vandoeuvre les Nancy CEDEX, France. E-mail: lecomte@lcm3b.u-nancy.fr

(*Received 30 April 1997; accepted 26 November 1997*)

Abstract

The experimental electron density distribution in triglycine has been determined using single-crystal X-ray diffraction data at 123 K to a resolution of $(\sin\theta/\lambda)_{max}$ = 1.1 Å^{-1}. Several multipolar pseudo-atom density refinements were performed against the 7238 observed data in order to estimate the net charges on the atoms. The electrostatic potential around the two molecules is calculated from the parameters derived from these refinements. A charge transfer between the two triglycine molecules of the asymmetric unit is discussed. Crystal data: $C_6H_{11}N_3O_4$, M_r = 189.2, triclinic, $P\bar{1}$, Z = 4 (two molecules in the asymmetric unit), T = 123 K, a = 11.585 (1), b = 14.603 (2), c = 4.800 (4) Å, α = 89.28 (3), β = 95.55 (2), γ = 104.484 (8)°, V = 782.5 (7) Å^3, D_x = 1.61 g cm^{-3}, μ = 1.5 cm^{-1} for λ_{Mo} = 0.7107 Å.

1. Introduction

We have been involved for many years in the high-resolution X-ray diffraction of amino acids (Souhassou *et al.*, 1991, 1992; Pichon-Pesme *et al.*, 1992; Wiest *et al.*, 1994; Lachekar *et al.*, 1998). In these papers we have described the electron density of the atoms with the most frequently used multipole formalism (Hansen & Coppens, 1978). These studies allowed us to show that the pseudo-atom aspherical scattering factors obtained can be transferable from one molecule to another (Pichon-Pesme *et al.*, 1995). These transferable pieces permit us to define more precisely the atomic scattering factors for any atom in a given chemical state and environment (C′, O, Cα, N *etc.*). Therefore, we decided to create a database of all the amino acid residues. This will enable us to refine high-resolution data of small proteins (Pichon-Pesme *et al.*, 1996). To improve our databank we report here the electron density distribution of triglycine.

The room-temperature crystal structure of triglycine was first established by Srikrishnan *et al.* (1982). In the crystal structure of triglycine the molecules are packed by means of numerous hydrogen bonds. Beside the electron density, the electrostatic potential will also be discussed.

2. Crystallographic analysis

2.1. *Data collection*

Triglycine was crystallized from water solution by solvent evaporation. A small crystal of the dimensions 0.3 × 0.2 × 0.04 mm was used to measure low-temperature Mo $K\alpha$ X-ray diffraction data on an Enraf–Nonius CAD-4F diffractometer equipped with a nitrogen-vapour stream apparatus and installed in a dry-box to prevent ice formation on the crystal. The gas stream temperature was maintained at 123 ± 2 K, as monitored by a copper–constantan thermocouple positioned ~5 cm upstream from the crystal. The homogeneity of the beam from the graphite incident-beam monochromator was measured and the intensity varied by less than 10% over the area intercepted by the specimen crystal. Lattice parameters were obtained by least-squares fit to the optimized setting angles of the $K\alpha_1$ peaks of 20 reflections with $30 < 2\theta < 40°$. Intensity data were recorded as ω–2θ scan profiles to a resolution of $\sin\theta/\lambda$ = 1.10 Å^{-1} for a total of 21 145 reflections in the following way: for $\sin\theta/\lambda$ < 0.8 Å^{-1} 3 equiv. were collected; after a conventional refinement against these low-order data, high-angle intensities were calculated to $\sin\theta/\lambda$ = 1.10 Å^{-1} and for those with an estimated $I > 6\sigma(I)$ intensities were measured once or twice at different values of ψ. During the data collection five standard reflections ($\bar{2}\bar{4}1$, $\bar{1}\bar{2}1$, 250, $\bar{8}\bar{5}1$ and 201) were measured at 3 h intervals. The total scan width ($\Delta\omega$) was 1.00 + 0.35° tan θ, with a constant detector aperture of 6 × 4 mm^2. A prescan speed $v = d\omega/dt$ of 2.75° min^{-1} and a final scan speed depending on the signal-to-noise ratio ($0.87 < v < 2.75°$ min^{-1}) were used for the low-angle data collection. The high-angle data were measured at a constant scan speed (0.87° min^{-1}). The total exposure time was 756 h. During the whole experiment no real problem associated with the crystal, temperature or diffractometer occurred.

2.2. *Data processing*

Data reduction and error analysis were performed using the programs of Blessing (1989). Reflection integration limits were from a Lorentzian model of the peak-width variations for high-order data and Gaussian

ISSN 0108-7681

Table 1. *Least-squares refinement statistics of fit*

$s = \sin\theta/\lambda$; $R = \Sigma(|F_o| - K|F_c|)/\Sigma|F_o|$; $wR = (\chi^2/\Sigma w|F_o|^2)^{1/2}$; $\chi^2 = \Sigma w(|F_o| - K|F_c|)^2$; $w = \sigma^{-2}(|F_o|)$; $S = [\chi^2/(n-m)]^{1/2}$; n data, m parameters; K is the scale factor.

Refinement	s (Å^{-1})	R	wR	S	K	m	n	Type
A	$0.8 < s < 1.1$	0.0287	0.0305	0.97	0.468	235	1925	Spherical
B	$s < 0.8$	0.0421	0.0500	2.29	0.482	89	5313	Spherical
C	$s < 1.1$	0.0256	0.0286	1.24	0.483	465	7238	Multipolar
D	$s < 1.1$	0.0255	0.0283	1.22	0.486	513	7238	Multipolar
E	$s < 1.1$	0.0248	0.0257	1.14	0.486	857	7238	Multipolar
F	$s < 1.1$	0.0246	0.0251	1.12	0.486	857	7238	Multipolar
G	$s < 1.1$	0.0387	0.0463	1.95	0.484	97	7238	Kappa

for low-order data. A polynomial fit to the smooth decline of ~3% in the standard reflections intensities over X-ray exposure was used to scale the data and to derive the instrumental instability coefficient $p = 0.022$ for the calculation of $\sigma^2(|F|^2) = \sigma_c^2(|F|^2) + (p|F|^2)^2$, with σ_c^2 propagation of error calculations. No absorption correction was performed.

The 21 145 reflections with $\sin\theta/\lambda < 1.10$ Å^{-1} were symmetry-averaged to 7238 independent data. Internal agreement, as defined in our previous studies (see, for example, Wiest *et al.*, 1994), were $R(F^2) = 0.0184$, $wR(F^2) = 0.0357$, $R^2(F^2) = 0.0110$ for all data and 0.0116, 0.0194 and 0.0103 for the 1745 unique data with $\sin\theta/\lambda <$ 0.5 Å^{-1}. The low value of the agreement factors for all data also shows that the high-order data were measured with a high accuracy.

2.3. *Least-squares refinements*

The crystal structure at room temperature was known from Srikrishnan *et al.* (1982). However, the low-temperature crystal structure was solved with *SHELXS*86 (Sheldrick, 1990). H atoms were found by difference-Fourier synthesis and refined isotropically against the low-order data. The bound-atom form factor for hydrogen (Stewart *et al.*, 1965), the form factor for the non-H atoms, calculated from Clementi & Raimondi (1963) wavefunctions, and the real and imaginary dispersion corrections to the form factors given by Cromer (1974) were used in the structure-factor calculations. The deformation density refinement was made on F^2 with the Hansen & Coppens (1978) model.

Fig. 1 gives the local coordinate system used in the multipolar refinement and the numbering scheme, and Fig. 2 is the *ORTEP*II view (Johnson, 1976) of the asymmetric unit: as two triglycine molecules exist in the asymmetric unit, the first digit (1 or 2) refers to the molecule number. First the xyz parameters, the anisotropic displacement parameters of the non-H atoms and the scale factor were refined against high-order data (refinement A), then xyz and the isotropic displacement motion parameters of the H atoms (refinement B) were refined. The coordinates of the H atoms were adjusted by extending along Csp^3—H and N—H, respectively, to 1.085 and 1.032 Å, which equal the average values from neutron diffraction (Allen, 1986). The H-atom coordinates and the isotropic displacement parameters were kept fixed during the whole refinement. Several types of refinement were performed. All statistics-of-fit are given in Table 1. At the beginning of the multipolar refinement, in order to reduce the number of variables, symmetry and chemical constraints were applied to the atoms and the two molecules in the asymmetric unit were kept identical (refinement C). Owing to the good quality of the data [all data have I greater than $2\sigma(I)$], the chemical and symmetry constraints were released (refinement D). In the third multipolar refinement (E) each triglycine molecule was refined separately, but constrained to remain neutral. The refinement of the (P_v, $P_{\rm lm}$) density parameters was therefore carried out molecule by molecule (refinement E). The total number of parameters, including 323 position and displacement variables, was 831, *i.e.* approximately 8.7 structure factors per least-square variable. The total number of parameters for refinement E is almost twice that of refinement D, and the agreement factors decrease but not dramatically; this is in agreement with our previous work (Pichon-Pesme *et al.*, 1995) on the equality between electron density multipole parameters of the same type of atoms in the same chemical environment. The last refinement (F) allowed charge transfer between the two triglycine molecules. This transfer may account for the numerous hydrogen bonds. Refinement F was performed with initial parameters E, refining both molecules together without any constraint. This last refinement converged to slightly better statistics-of-fit than refinement E (see Table 1). Refinements E and F led to the same residual density map. Maximum residuals (0.2 e Å^{-3}) are found close to the N-terminal

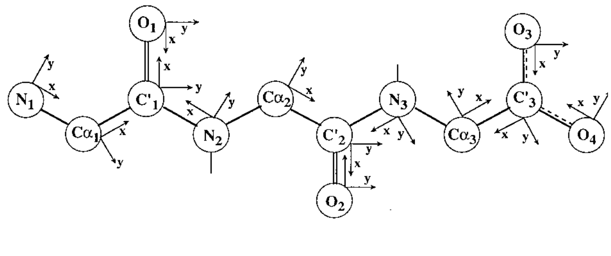

Fig. 1. Numbering scheme and local coordinate system for triglycine.

extremity (HN11). Multipolar and displacement parameters of both refinements are equal within standard deviations. The largest change concerns, as expected, the P_v parameters: when charge transfer between molecule 1 and molecule 2 is allowed, the P_v parameters of the two carboxyl C atoms change by 0.18 e (Table 2), while the other atoms show changes in P_v of less than 0.08 e. The resulting net charge on each molecule is $q = +0.74$ e for molecule 1 and $q = -0.74$ e for molecule 2 compared with the lowest e.s.d. calculated from

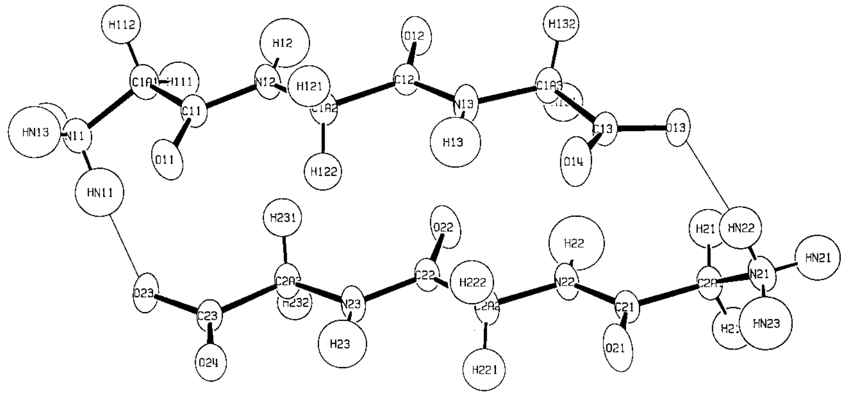

Fig. 2. *ORTEP*II (Johnson, 1976) view of the asymmetric unit.

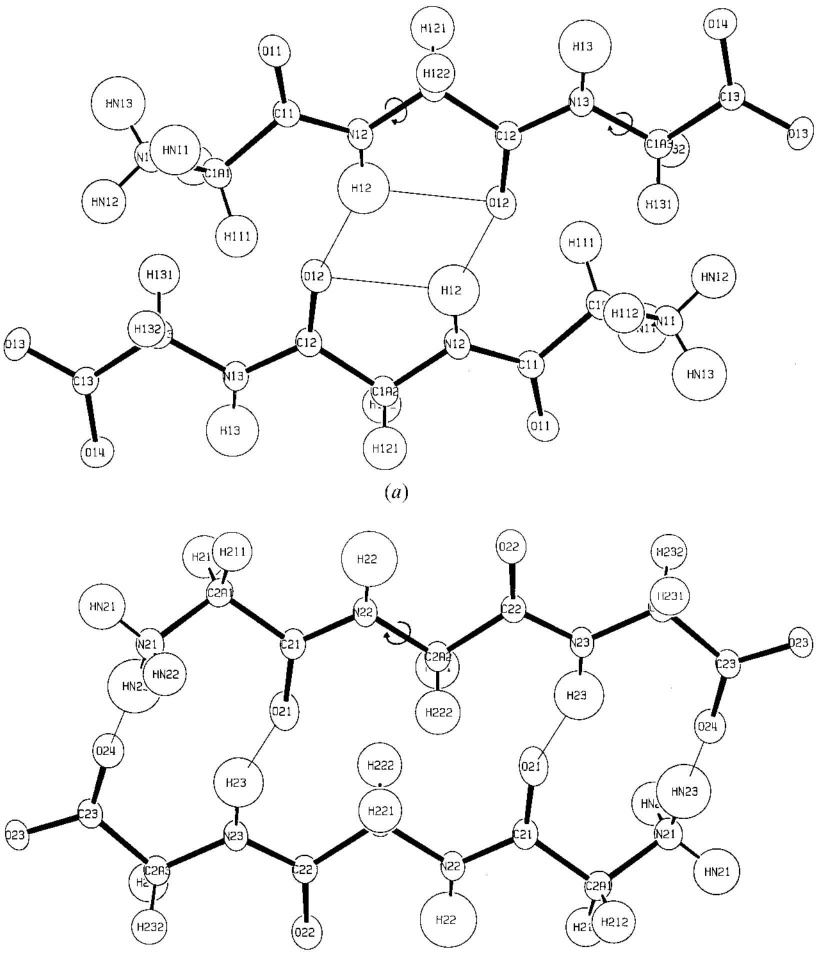

Fig. 3. *ORTEP*II (Johnson, 1976) view of the dimer of (*a*) molecule 1 and (*b*) molecule 2. The rotating arrow shows the libration axis.

Table 2. *Net charges (e) of atoms after refinements D, E and F with e.s.d.'s in parentheses*

	D	*E*	*F*
N11	−0.68 (2)	−0.75 (3)	−0.71 (3)
N21	−0.68 (2)	−0.67 (3)	−0.73 (3)
C1*A*1	−0.25 (2)	−0.14 (3)	−0.07 (4)
C2*A*1	−0.25 (2)	−0.23 (4)	−0.28 (4)
C11	+0.10 (2)	+0.19 (3)	+0.21 (3)
C21	+0.10 (2)	+0.01 (3)	−0.04 (3)
O11	−0.32 (1)	−0.28 (2)	−0.25 (2)
O21	−0.32 (1)	−0.40 (2)	−0.42 (2)
N12	−0.42 (2)	−0.33 (2)	−0.33 (3)
N22	−0.42 (2)	−0.38 (3)	−0.40 (3)
C1*A*2	−0.32 (2)	−0.27 (4)	−0.22 (4)
C2*A*2	−0.32 (2)	−0.43 (4)	−0.38 (4)
C12	+0.08 (2)	+0.10 (3)	+0.13 (3)
C22	+0.08 (2)	+0.05 (3)	+0.04 (3)
O12	−0.28 (1)	−0.31 (2)	−0.32 (2)
O22	−0.28 (1)	−0.33 (2)	−0.38 (2)
N13	−0.42 (2)	−0.44 (3)	−0.39 (3)
N23	−0.42 (2)	−0.44 (3)	−0.45 (3)
C1*A*3	−0.18 (2)	−0.30 (4)	−0.21 (4)
C2*A*3	−0.18 (2)	−0.02 (3)	−0.08 (4)
C13	−0.15 (3)	−0.50 (4)	−0.32 (4)
C23	−0.15 (3)	+0.05 (4)	−0.13 (4)
O13	−0.50 (1)	−0.58 (2)	−0.54 (2)
O23	−0.50 (1)	−0.40 (2)	−0.44 (2)
O14	−0.43 (2)	−0.36 (2)	−0.31 (2)
O24	−0.43 (2)	−0.40 (2)	−0.38 (2)
HN11	+0.50 (1)	+0.53 (2)	+0.54 (2)
HN21	+0.50 (1)	+0.49 (2)	+0.49 (2)
HN12	+0.50 (1)	+0.58 (2)	+0.52 (2)
HN22	+0.50 (1)	+0.49 (2)	+0.47 (2)
HN13	+0.50 (1)	+0.54 (2)	+0.56 (2)
HN23	+0.50 (1)	+0.44 (2)	+0.42 (2)
H111	+0.25 (1)	+0.26 (2)	+0.30 (2)
H211	+0.25 (1)	+0.28 (2)	+0.27 (2)
H112	+0.25 (1)	+0.22 (2)	+0.21 (2)
H212	+0.25 (1)	+0.24 (2)	+0.20 (2)
H12	+0.39 (1)	+0.43 (2)	+0.45 (2)
H22	+0.39 (1)	+0.38 (2)	+0.36 (2)
H121	+0.25 (1)	+0.23 (2)	+0.26 (2)
H221	+0.25 (1)	+0.23 (2)	+0.15 (2)
H122	+0.25 (1)	+0.31 (2)	+0.30 (2)
H222	+0.25 (1)	+0.23 (2)	+0.20 (2)
H13	+0.39 (1)	+0.46 (2)	+0.48 (2)
H23	+0.39 (1)	+0.40 (2)	+0.37 (2)
H131	+0.25 (1)	+0.24 (2)	+0.23 (2)
H231	+0.25 (1)	+0.23 (2)	+0.24 (2)
H132	+0.25 (1)	+0.22 (2)	+0.22 (2)
H232	+0.25 (1)	+0.21 (2)	+0.17 (2)

$$\sigma(q) = (\Sigma\sigma_i^2(P_v))^{1/2} = 0.13\ \text{e},$$

where *i* runs over all atoms of the molecule. The net charge obtained is only 5.7σ. This charge transfer could be attributed to the hydrogen bonds existing between molecules 1 and 2 (see later). A similar molecular net charge was also obtained from a kappa refinement (*G*) performed at the end of refinement *E* (±0.78 e). The convergence of all refinements was reached without correlation greater than 0.8 between P_v parameters even for refinement *F* (no constraints). In all the refinements no extinction refinement was deemed necessary. Table 3 gives the fractional coordinates of all the atoms (refinement *F*). Bond distances and angles are listed Table 4.†

Table 3. *Fractional atomic coordinates and equivalent isotropic displacement parameters (Å^2)*

For non-H atoms $U_{\rm eq} = (1/3)\Sigma_i\Sigma_j U^{ij}a^i a^j \mathbf{a}_i.\mathbf{a}_j$.

	x	*y*	*z*	$U_{\rm eq}$
N11	0.05709 (4)	0.43464 (3)	−0.25627 (8)	0.011
C1*A*1	0.18475 (4)	0.43518 (3)	−0.21362 (10)	0.011
C11	0.25325 (4)	0.50773 (3)	−0.40770 (9)	0.010
O11	0.20007 (3)	0.53920 (3)	−0.60722 (8)	0.014
N12	0.37126 (4)	0.53489 (3)	−0.34016 (8)	0.011
C1*A*2	0.44715 (4)	0.60839 (3)	−0.49257 (10)	0.011
C12	0.56896 (4)	0.63978 (3)	−0.32601 (9)	0.010
O12	0.59351 (3)	0.59916 (3)	−0.10874 (8)	0.014
N13	0.64619 (4)	0.71253 (3)	−0.43117 (8)	0.012
C1*A*3	0.76322 (4)	0.75381 (3)	−0.28598 (10)	0.011
C13	0.82693 (4)	0.84327 (3)	−0.43166 (9)	0.010
O13	0.92017 (3)	0.89396 (2)	−0.29900 (7)	0.012
O14	0.78515 (4)	0.85933 (3)	−0.67100 (8)	0.018
N21	0.93357 (4)	1.08954 (3)	−0.18906 (8)	0.012
C2*A*1	0.83681 (4)	1.05025 (3)	−0.00831 (10)	0.010
C21	0.71962 (4)	1.01438 (3)	−0.18722 (10)	0.010
O21	0.69906 (4)	1.05279 (3)	−0.41097 (8)	0.019
N22	0.64162 (4)	0.94118 (3)	−0.08640 (8)	0.011
C2*A*2	0.52556 (4)	0.90673 (3)	−0.2395 (1)	0.012
C22	0.44777 (4)	0.82691 (3)	−0.08556 (9)	0.010
O22	0.48747 (3)	0.78941 (3)	0.12179 (8)	0.016
N23	0.33394 (4)	0.80054 (3)	−0.19841 (8)	0.011
C2*A*3	0.24529 (4)	0.72462 (3)	−0.08709 (10)	0.011
C23	0.12894 (4)	0.70332 (3)	−0.27958 (9)	0.010
O23	0.04771 (3)	0.63125 (2)	−0.21562 (7)	0.012
O24	0.11766 (3)	0.75462 (3)	−0.48350 (8)	0.014
HN11	0.05202	0.50428	−0.26255	0.027
HN12	0.00799	0.39455	−0.10911	0.021
HN13	0.01548	0.40536	−0.44554	0.031
H111	0.21474	0.45336	0.00458	0.019
H112	0.19353	0.36492	−0.26091	0.017
H12	0.40623	0.50562	−0.16528	0.028
H121	0.45850	0.58429	−0.69846	0.020
H122	0.40599	0.66739	−0.51813	0.016
H13	0.62139	0.74610	−0.60887	0.023
H131	0.75424	0.77292	−0.07296	0.017
H132	0.82214	0.70645	−0.28613	0.014
HN21	1.01155	1.11289	−0.05874	0.023
HN22	0.94354	1.03459	−0.31016	0.020
HN23	0.91769	1.14210	−0.32160	0.032
H211	0.85993	0.99468	0.12009	0.017
H212	0.82858	1.10501	0.13387	0.020
H22	0.66548	0.90669	0.09062	0.034
H221	0.48103	0.96399	−0.25711	0.021
H222	0.53771	0.88131	−0.44322	0.021
H23	0.30727	0.83523	−0.37173	0.027
H231	0.27858	0.66152	−0.06611	0.017
H232	0.22400	0.74236	0.11739	0.014

† Lists of anisotropic displacement parameters, structure factors and the density parameters from refinement *F*, and electron density maps have been deposited with the IUCr (Reference: BS0002). Copies may be obtained through The Managing Editor, International Union of Crystallography, 5 Abbey Square, Chester CH1 2HU, England.

3. Results and discussion

3.1. *Molecular conformation*

The *b* parameter decreases significantly during cooling (1.5%) and the relative variation of the unit cell volume is 2%, but the conformation of triglycine remains identical. Fig. 2 shows the conformation of the two independent molecules of the asymmetric unit. These two molecules have an extended planar conformation and are packed in a head-to-tail fashion. All conformation angles are mostly equal to 180°, except for the φ angle involving the N-terminal in molecule 2 [φ = N21—C2*A*1—C21—N22 = 149.3 (4)°]. Indeed, this N atom (N21) and the O atom (O21) form an intramolecular hydrogen bond [N···O = 2.7438 (6) Å]. The geometry of the intermolecular hydrogen bonding has been described extensively by Srikrishnan *et al.* (1982) and we refer the reader to this paper. Each COO^-, NH_3^+, CO and NH group is involved in at least one hydrogen bond (single or bifurcated). As a consequence, the density of this compound is high (1.61 g cm^{-3} at 123 K, 1.58 g cm^{-3} at room temperature). The intermolecular hydrogen-bond distances decrease an average of 1% when the crystal is cooled down to 123 K. Hydrogen bonds at room temperature and 123 K are listed in Table 5.

3.2. *Thermal vibration analysis*

The Hirshfeld rigid-bond test (Hirshfeld, 1976) was carried out on both molecules. All mean square displacement amplitudes along bond directions differed by less than 0.001 Å^2, indicating that the multipole refinement yielded an effective deconvolution of the mean-square atomic displacements from the valence electron density deformation. The *THMA*11 program of Trueblood (1990) was used to perform *TLS* + φ analysis on the two individual molecules. The results are given in Table 6. Molecule 2 appears to be more rigid than molecule 1: hence, molecule 1 forms a centrosymmetric dimer by means of two H12···O12 hydrogen bonds, leading to a ten-membered ring (Fig. 3*a*), which allows the non-rigid motion of both N-terminal and C-terminal residues. This is not the case for molecule 2, which forms a dimer by means of two ten-membered rings involving COO and NH_3 residues (Fig. 3*b*).

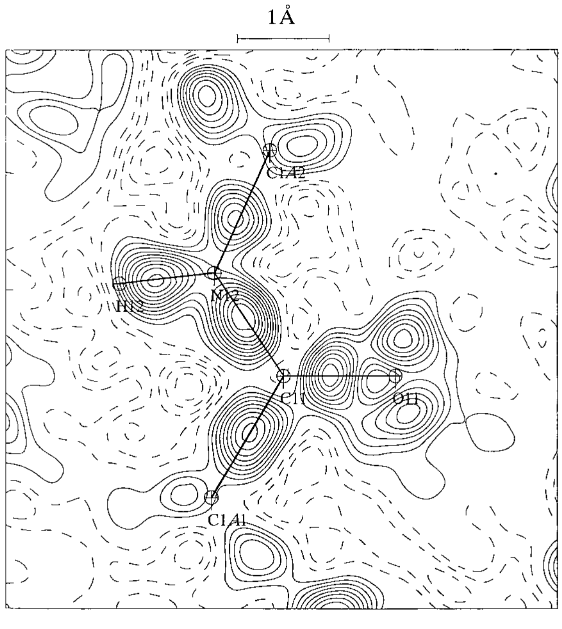

Fig. 4. Experimental deformation electron density of one peptide group. Contour interval 0.05 e Å^{-3}; positive solid line, negative dashed line, zero contour omitted.

Table 4. *Selected geometric parameters (Å, °)*

N11—C1*A*1	1.4714 (6)	N21—C2*A*1	1.4806 (6)
C1*A*1—C11	1.5224 (6)	C2*A*1—C21	1.5117 (6)
C11—O11	1.2347 (6)	C21—O21	1.2357 (6)
C11—N12	1.3334 (6)	C21—N22	1.3348 (6)
N12—C1*A*2	1.4466 (6)	N22—C2*A*2	1.4426 (6)
C1*A*2—C12	1.5193 (6)	C2*A*2—C22	1.5161 (6)
C12—O12	1.2376 (6)	C22—O22	1.2351 (6)
C12—N13	1.3350 (6)	C22—N23	1.3393 (6)
N13—C1*A*3	1.4512 (6)	N23—C2*A*3	1.4461 (6)
C1*A*3—C13	1.5280 (6)	C2*A*3—C23	1.5244 (6)
C13—O13	1.2646 (5)	C23—O23	1.2804 (5)
C13—O14	1.2457 (6)	C23—O24	1.2419 (6)
N11—C1*A*1—C11	108.69 (4)	N21—C2*A*1—C21	109.77 (4)
O11—C11—N12	124.12 (4)	O21—C21—N22	123.31 (4)
O11—C11—C1*A*1	120.79 (4)	O21—C21—C2*A*1	120.62 (4)
N12—C11—C1*A*1	115.07 (4)	N22—C21—C2*A*1	116.07 (4)
C11—N12—C1*A*2	121.44 (4)	C21—N22—C2*A*2	118.87 (4)
N12—C1*A*2—C12	108.75 (4)	N22—C2*A*2—C22	111.12 (4)
O12—C12—N13	123.16 (4)	O22—C22—N23	123.84 (4)
O12—C12—C1*A*2	121.25 (4)	O22—C22—C2*A*2	122.42 (4)
N13—C12—C1*A*2	115.59 (4)	N23—C22—C2*A*2	113.73 (4)
C12—N13—C1*A*3	121.69 (4)	C22—N23—C2*A*3	122.71 (4)
N13—C1*A*3—C13	111.00 (4)	N23—C2*A*3—C23	110.46 (4)
O14—C13—O13	125.44 (4)	O24—C23—O23	124.18 (4)
O13—C13—C1*A*3	116.46 (4)	O24—C23—C2*A*3	119.97 (4)
O14—C13—C1*A*3	118.07 (4)	O23—C23—C2*A*3	115.85 (4)

3.3. *Electron density*

The experimental deformation electron density of one peptide group is shown in Fig. 4, calculated from

$$\delta\rho(\mathbf{r}) = V^{-1}\Sigma(|F_o|\exp(i\varphi_m) - |F_s|\exp(i\varphi_s))\exp(-2\pi i\mathbf{Hr}),$$

where F_o and F_s are observed and spherical structure-factor amplitudes, respectively, and φ_m and φ_s are the multipolar and spherical phases, respectively. The sum is over all observed structure factors [with a resolution of $(\sin\theta/\lambda)_{max}$ = 0.9 Å^{-1}]. The deformation maps of the other peptides groups maps look very similar.† Positive

† See deposition footnote on p. 488.

Table 5. *Hydrogen bond distances (Å) and angles (°) from this study (refinement F) at 123 K and from a previous study at room temperature, values in italic (Srikrishnan et al., 1982)*

D—H···A	D···A	H···A	D—H—A
N11—HN12···O23^{i}	2.7246 (5)	1.7453 (4)	156.75 (2)
	2.733	*1.77*	*163*
N11—HN13···O23^{ii}	2.7762 (5)	1.7501 (3)	173.14 (2)
	2.789	*1.71*	*172*
N11—HN11···O23^{iii}	2.9098 (6)	1.8841 (4)	171.46 (2)
	2.941	*1.99*	*172*
N21—HN21···O13^{iv}	2.7312 (5)	1.8322 (3)	143.40 (2)
	2.749	*1.86*	*143*
N21—HN23···O21^{iii}	2.7438 (6)	2.5400 (4)	89.35 (1)
	2.744	*2.53*	*93*
N21—HN22···O13^{iii}	2.8740 (6)	2.0039 (4)	140.18 (2)
	2.925	*2.18*	*140*
N21—HN23···O24^{v}	2.8994 (6)	1.8753 (4)	171.61 (3)
	2.913	*1.98*	174
N12—H12···O12^{iii}	2.6472 (5)	2.2494 (4)	101.00 (2)
	2.658	*2.26*	*108*
N12—H12···O12^{vi}	2.9606 (6)	2.0056 (4)	152.83 (2)
	2.991	*2.20*	*152*
N13—H13···O14^{iii}	2.6613 (5)	2.2249 (4)	103.48 (2)
	2.663	*2.30*	*104*
N13—H13···O22^{vii}	3.0749 (6)	2.1356 (4)	150.46 (3)
	3.107	*2.28*	*156*
N22—H22···O22^{iii}	2.7220 (5)	2.3442 (3)	100.10 (2)
	2.729	*2.39*	*103*
N22—H22···O14^{viii}	2.9089 (6)	1.9653 (4)	150.58 (3)
	2.940	*2.12*	*153*
N23—H23···O21^{v}	2.9016 (6)	1.9416 (4)	153.68 (2)
	2.292	*2.07*	*156*
N23—H23···O24^{iii}	2.6683 (5)	2.2346 (3)	103.36 (2)
	2.676	*2.27*	*107*

Symmetry codes: (i) $-x, 1-y, -z$; (ii) $-x, 1-y, -1-z$; (iii) x, y, z; (iv) $2-x, 2-y, -z$; (v) $1-x, 2-y, -1-z$; (vi) $1-x, 1-y, -z$; (vii) $x, y, -1+z$; (viii) $x, y, 1+z$.

densities are observed along valence bonds and the O-atom lone pairs show up. The bonding maxima are located between the nuclei and their heights are summarized in Table 7 compared with those obtained on Leu-enkephalin dihydrate (Wiest *et al.*, 1994) and *N*-acetyl-α,β-dehydrophenylalanine methylamide (Souhassou *et al.*, 1992). A very good agreement within estimated σ (0.05 e Å^{-3}) is observed. The two distinct lobes in the oxygen lone pair are better resolved than in our previous study of Leu-enkephalin; their height varies in the range 0.20–0.40 e Å^{-3}. The static electron density† also agrees with our previous work and *ab initio* SCF (self-consistence field) calculation (Souhassou *et al.*, 1992).

3.4. *Electrostatic potential*

The electrostatic potential was calculated using the *Electros* program (Ghermani *et al.*, 1992) for each molecule considered as a pseudo-isolated entity removed from the crystal lattice. Figs. 5(*a*) and 5(*b*) show the electrostatic potential of each molecule of the asymmetric unit in the N12, O12, C12 (N22, O22, C22) plane calculated from refinement *D*, *i.e.* both molecules

† See deposition footnote on p. 488.

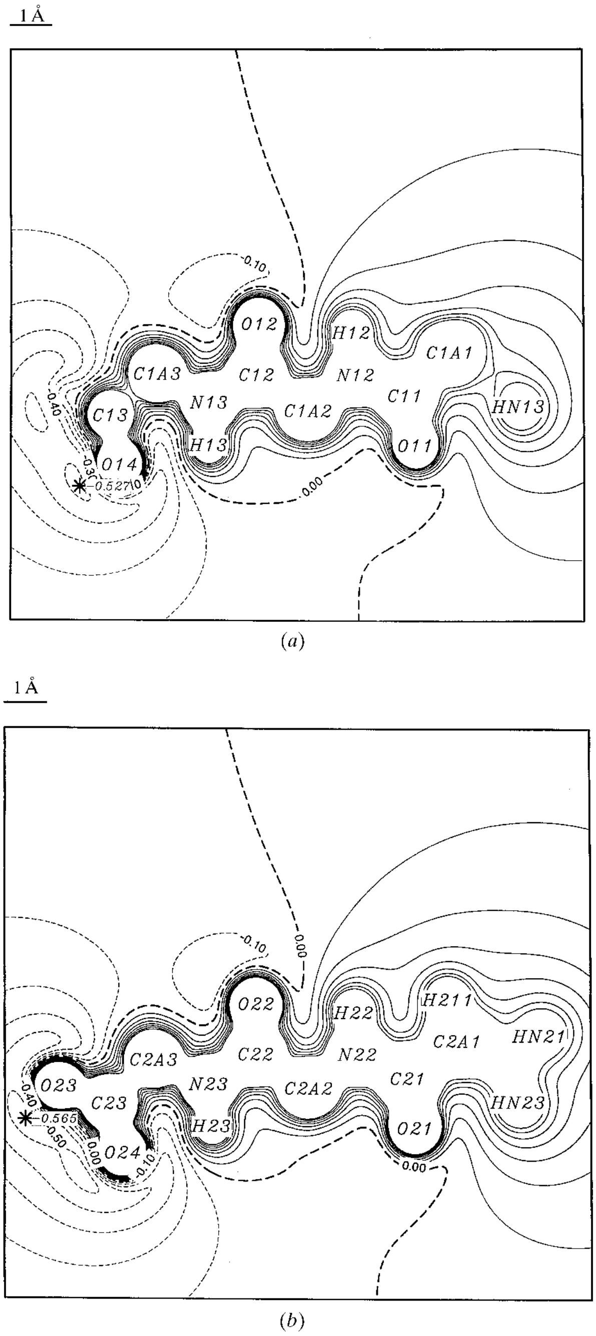

Fig. 5. Electrostatic potential of the two molecules in the planes (*a*) N12, O12, C12 and (*b*) N22, O22, C22 after refinement *D*. Contour interval 0.10 e Å^{-1}; positive solid line, negative dashed line, zero contour as broken lines.

Table 6. *Thermal vibration analysis*

	Molecule 1		Molecule 2	
	Rigid	Flexible	Rigid	Flexible
R†	0.111	0.076	0.102	0.073
n observations	78	78	78	78
m parameters	20	32	20	26

Librating group	Libration axis	$\langle\varphi^2\rangle$ (°^{2})	Force constant (J mol^{-1} deg^{-2})
C13—O13—O14	N13—C1*A*3	29.4 (6.0)	35.6 (6.1)
N11—C1*A*1—C11—O11	N12—C1*A*2	14.9 (4.9)	71.8 (18.3)
N21—C2*A*1—C21—O21	N22—C2*A*2	10.6 (4.9)	100.3 (33.8)

† For a definition of the *R* factor see Souhassou *et al.* (1991).

were constrained to have the same electron density. As expected, the potential around the two molecules is the same, with negative potential around the negative carboxyl groups. The differences observed are only due to the slightly different conformation of both triglycine molecules. We note that the potential around O11 (O21) is almost zero, even though the oxygen charge is −0.32 e: indeed, these carbonyl atoms are very close to the electropositive area due to the presence of NH_3^+ groups.

Figs. 6(*a*), 6(*b*), 7(*a*) and 7(*b*) show the potential calculated in the same planes from refinements *E* and *F*. In refinement *E*, in which only the electroneutrality of each individual molecule is imposed, the electrostatic potential changes by ~0.1 e Å^{-1} around the carboxyl group compared with that calculated from refinement *D* and we observe a slightly more negative area around O21. This difference increases when we use the parameters of refinement *F*: molecule 1 (Fig. 7*a*) appears to be less negative than molecule 2 in the carboxyl group region, in agreement with the net charges of both molecules (±0.74 e).

4. Conclusions

The overall picture of the electrostatic potential and charge density is the same for all refinements, but a closer examination shows that the resulting electrostatic properties derived from this electron density study can be very much dependent on the refinement strategy. The problem is to know which of the three refinements performed is the closest to reality. On the one hand, as both triglycine molecules are almost in the same conformation, we expect very similar charges for each molecule. This is in agreement with the transferability of electron density parameters which we published a year ago. On the other hand, there are many hydrogen bonds (see Table 5) linking together molecule 1 to molecule 1, molecule 2 to molecule 2 and molecule 1 to molecule 2. Some of these are strong (N···O = 2.70 Å) enough to involve charge transfer between molecules. This could explain the result of the refinement *F*, but the net charge of each triglycine molecule appears to be too large (±0.74 e) compared with the charge transfer found, for example, in the one-dimensional metal BTDMTF-

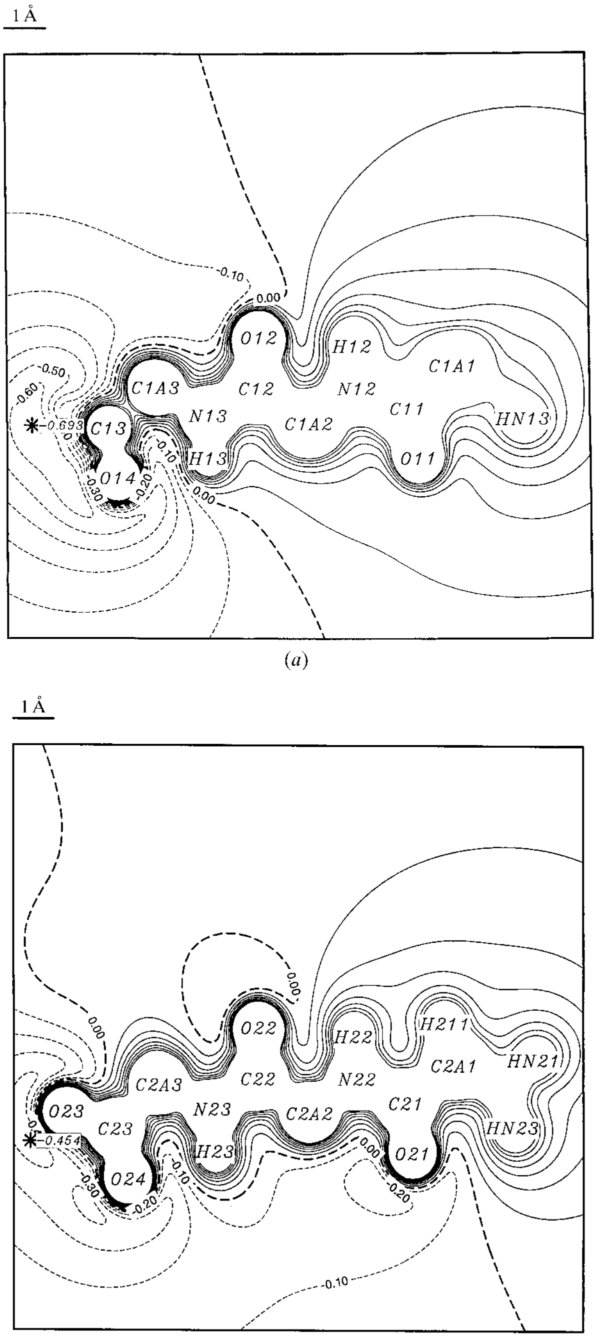

(*a*)

(*b*)

Fig. 6. As in Fig. 5 after refinement *E*.

TCNQ at 130 K [0.7 e by charge density refinement (Espinosa *et al.*, 1997) and 0.6 e by diffuse scattering experiment (Rovira *et al.*, 1995)]. Therefore, as (*a*) the statistical indices for both refinements *E* and *F* are almost equal (Table 1), (*b*) the hydrogen bonds involved in the formation of dimers between molecules 1 and molecules 2 are almost balanced in the sense that the number of NH donor groups is the same for each molecule (Table 5), and (*c*) the minimum e.s.d. on the total charge of triglycine is 0.13 e, the results of refinement *E* seem to be the most reliable. However, in order to solve this problem, we are performing refinements using model structure factors calculated from refinements *E* and *F*. The results will be published later.

Table 7. *Experimental deformation electron density peaks (e Å^{-3}) in triglycine for the four peptide bonds*

	C′=O	C′−N	C′−Cα	Cα−N	N−H
N12−C11−O11	0.45	0.50	0.45	0.35	0.50
N13−C12−O12	0.55	0.40	0.45	0.35	0.45
N22−C21−O21	0.45	0.45	0.50	0.35	0.50
N23−C22−O22	0.55	0.40	0.40	0.30	0.50
<Trig>†	0.50	0.44	0.45	0.34	0.49
<Enk>‡	0.50	0.49	0.38	0.30	0.40
AcΔ§	0.57	0.50	0.47	0.36	0.47

† Average values of triglycine. ‡ Average values of leu-enkephalin (Wiest *et al.*, 1994). § Average values of *N*-acetyl-α,β-dehydrophenylalanine methylamide (Souhassou *et al.*, 1992).

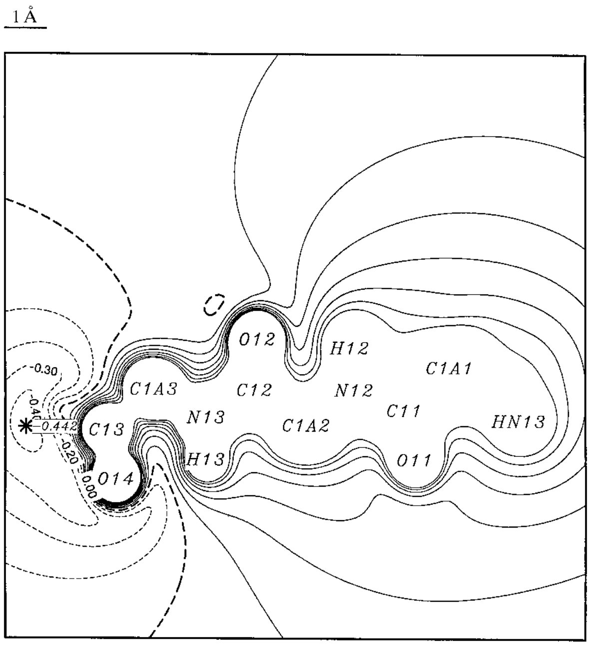

(*a*)

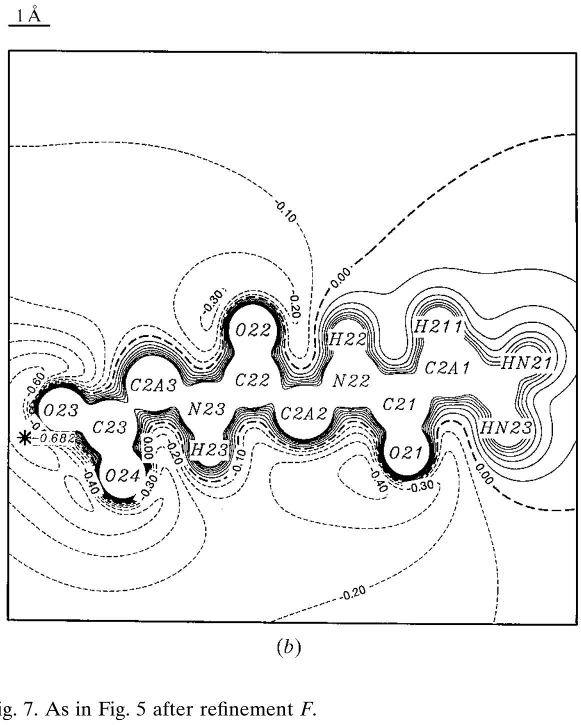

(*b*)

Fig. 7. As in Fig. 5 after refinement *F*.

The authors thank Dr Enrique Espinosa for helping during the data collection. VPP is grateful for the hospitality of Professor P. Coppens during a 6 month postdoctoral position and NATO for a postdoctoral fellowship (1993).

References

Allen, F. (1986). *Acta Cryst.* B**42**, 515–522.
Blessing, R. H. (1989). *J. Appl. Cryst.* **22**, 396–397.
Clementi, E. & Raimondi, D. L. (1963). *J. Chem. Phys.* **41**, 2686–2689.
Cromer, D. T. (1974). *International Tables for X-ray Crystallography*, eidted by J. A. Ibers & W. E. Hamilton, pp. 148–151. Birmingham: Kynoch Press. (Present distributor Kluwer Academic Publishers, Dordrecht.)
Espinosa, E., Molins, E. & Lecomte, C. (1997). *Phys. Rev. B*, **56**, 1820–1833.
Ghermani, N.-E., Bouhmaida, N. & Lecomte, C. (1992). *ELECTROS. Computer Program to Calculate Electrostatic Properties from High Resolution X-ray Diffraction.* Internal report URA CNRS 809. University of Nancy 1, France.
Hansen, N. K. & Coppens, P. (1978). *Acta Cryst.* A**34**, 909–921.
Hirshfeld, F. L. (1976). *Acta Cryst.* A**32**, 239–244.
Johnson, C. K. (1976). *ORTEP*II. Report ORNL-5138. Oak Ridge National Laboratory, Tennessee, USA.
Lachekar, H., Pichon-Pesme, V. & Lecomte, C. (1998). *Acta Cryst.* Submitted.
Pichon-Pesme, V., Lecomte, C. & Lachekar, H. (1995). *J. Phys. Chem.* **99**, 6242–6250.

Pichon-Pesme, V., Lecomte, C., Wiest, R. & Bénard, M. (1992). *J. Am. Chem. Soc.* **114**, 2713–2715.
Pichon-Pesme, V., Lachekar, H. & Lecomte, C. (1996). International Union of Crystalography Congress, Seattle, Washington, USA.
Rovira, C., Tarrés, J., Llorca, J., Molins, E., Jeciana, J., Yang, J., Cowan, D. O., Garrigou-Lagrange, C., Amiell, J., Delhoes, P., Canadell, E. & Poujet, J. P. (1995). *Phys. Rev.* **52**, 8747–8758.
Sheldrick, G. M. (1990). *Acta Cryst.* A**46**, 467–473.
Souhassou, M., Lecomte, C., Blessing, R. H., Aubry, A., Rohmer, M.-M., Wiest, R. & Bénard, M. (1991). *Acta Cryst.* B**47**, 253–266.
Souhassou, M., Lecomte, C., Ghermani, N.-E., Rohmer, M.-M., Wiest, R., Bénard, M. & Blessing, R. H. (1992). *J. Am. Chem. Soc.* **114**, 2371–2382.
Stewart, R. F., Davidson, E. R. & Simpson, W. T. (1965). *J. Chem. Phys.* **43**, 175–187.
Srikrishnan, T., Winiewicz, N. & Parthasarathy, R. (1982). *Int. J. Pept. Protein Res.* **19**, 103–113.
Trueblood. K. N. (1990). *THMA*11. *Program for Thermal Motion Analysis*. University of California at Los Angeles, USA.
Wiest, R., Pichon-Pesme, V., Bénard, M. & Lecomte, C. (1994). *J. Phys. Chem.* **98**, 1351–1362.